JOURNAL OF CATALYSIS **169,** 307–316 (1997)
ARTICLE NO. CA971704

Fluorination of CF_3CH_2Cl over Cr–Mg Fluoride Catalyst: The Effect of Temperature on the Catalyst Deactivation

Hyunjoo Lee,* Hyun Dam Jeong,† Young Su Chung,† Han Gil Lee,† Moon Jo Chung,* Sehun Kim,† and Hoon Sik Kim*

*Korea Institute of Science and Technology, P.O. Box 131 Cheongrayng, Seoul 130-650, Korea; and †Department of Chemistry and Center for Molecular Science, Korea Advanced Institute of Science and Technology, Taejon 305-701, Korea

Received December 13, 1996; revised March 7, 1997; accepted March 7, 1997

The heterogeneous fluorination catalysts ($Cr(OH)_xF_{3-x}$), which have recently been employed for the synthesis of CF_3CH_2F (HFC-134a), were characterized by X-ray diffraction, infrared spectroscopy, and photoelectron spectroscopy. The IR study of these catalyst samples indicated that the amount of hydroxyl group in chromium phases decreases as the deactivation process proceeds. Pyridine adsorption experiments showed that these catalyst samples possess both Lewis and Brønsted acid sites and the strengths of Lewis acid sites diminish as the catalyst activity decreases. Elemental analyses and XPS revealed that the catalyst sample prepared at a higher reaction temperature contained larger amount of cokes that are believed to be the major cause of catalyst deactivation. The XPS analysis indicates that the carbon cokes appear to be carbidic carbons which are produced by the successive decomposition of reactants. *In situ* IR experiments were performed with CF_3CH_2Cl and $CF_2{=}CHCl$ to elucidate the pathway to coke formation. The activity quenching was observed for the alkali metal-doped catalyst, which supports the important role of Lewis acidity in the catalysis.

INTRODUCTION

Recently, it has been believed that chlorofluorocarbons (CFCs) used as coolants and aerosol propellants are responsible for depletion of the stratospheric ozone layer (1). The preparation of hydrofluorocarbons (HFCs) and hydrochlorofluorocarbons (HCFCs) attracts much attention as the alternatives of CFCs (1). Chromium and aluminum fluoride catalysts are widely used for the preparations of HFCs and HCFCs (1–5). Presently, we are studying a fluorination reaction to manufacture CF_3CH_2F (HFC-134a) from CF_3CH_2Cl (HCFC-133a) using chromium–magnesium fluoride catalysts.

In a previous paper, we reported that the addition of MgF_2 is effective in enhancing the fluorination activity and also in reducing the formation of undesired side products for the CrF_3-catalyzed fluorination reaction (6a). Various preparation methods were tested for the preparation of highly active CrF_3–MgF_2 catalyst. Among the catalysts tested, the catalyst prepared by alcohol reduction of CrO_3–MgF_2 solution exhibits the highest activity and the largest surface area. One of the most important factors in the commercialization of CF_3CH_2F by the heterogeneous fluorination reaction is the lifetime of the catalyst. In order to prolong the lifetime of the catalysts, we have been studying the deactivation phenomena occurring on the catalyst surfaces.

The deactivation of catalyst is believed to be mostly affected by the coke formation for the fluorination catalysis. *In situ* IR adsorption experiments were performed with CF_3CH_2Cl and $CF_2{=}CHCl$ to determine the nature of precursors responsible for the coke formation. The main purpose of this work is to attain a better understanding of catalyst deactivation by performing the fluorination reaction and by characterizing the structure and the composition of the catalysts by using X-ray diffraction, Fourier transform infrared spectroscopy (FT-IR), and X-ray photoelectron spectroscopy.

EXPERIMENTAL

Reagents

All reactant gases and reagents for the preparation of catalysts were commercially purchased and used as received without further purification.

Synthesis of Chromium–Magnesium Fluoride Catalysts

$Cr(OH)_3 \cdot H_2O$ was prepared by alcohol reduction of CrO_3 (7). $Cr(OH)_3 \cdot xH_2O/MgF_2$ (Cr/Mg = 1/4) was prepared in a manner similar to the preparation of $Cr(OH)_3 \cdot xH_2O$. Li- and K-doped catalysts were prepared by the impregnation of $Cr(OH)_3 \cdot xH_2O/MgF_2$ with LiCl or KF aqueous solution and subsequent drying at 140°C overnight. The resulting dried solid was powdered and formed into cylindrical pellets. The pelletized catalysts, prior to use, were subjected to the activation process which provides them with an activity for the fluorination of CF_3H_2Cl. The

0021-9517/97 $25.00

activation process of the catalysts was performed through *in situ* treatment with HF. Commercially purchased anhydrous CrF_3, $CrF_3 \cdot 3H_2O$, and $CrF_3 \cdot 4H_2O$ were also formed into pellets and pretreated as in the same way described above.

Catalyst Activation

The fluorination reactor was made of an Inconel 600 tubing of 1 in. diameter and 30 cm long equipped with an electrical heater. Thirty grams of catalyst was loaded into the reactor and dried *in situ* at 400°C for 1 h in He at a flow of 200 ml/min. The activation process was followed with 400 ml/min HF at 200°C for 2 h and subsequently at 400°C for 1 h.

Fluorination Reaction

The fluorination reactions were carried under an atmospheric pressure in a fixed-bed reactor. Effluent reaction mixture was analyzed by on-line Gaw-Mac 580P TCD GC equipped with a 6-f Porapak N column after being scrubbed with H_2O and dried over molecular sieve 4A. Flow rates of CF_3CH_2Cl and HF preheated in a chamber at 45°C were carefully controlled using Matheson mass flow controllers. The deactivated catalyst obtained from the fluorination reaction at 450°C was regenerated at 420°C in an air flow of 200 ml/min for 2 h.

Sample Preparations

Catalyst samples having different catalytic activities were prepared from the fluorination reactions carried out under the following conditions. Sample 1 was obtained from the fluorination reaction carried out at 340°C for 12 h. Samples 2 and 3 were prepared via the fluorination reactions performed at 400 and 450°C for 10 h, respectively and subsequently at 340°C for 2 h. Sample 3 was air regenerated at 420°C and fluorinated at 340°C for 12 h to give sample 4. Samples 5 and 6 were prepared from the fluorination reaction conducted at 340°C for 12 h with 0.5% Li- and K-doped chromium–magnesium fluoride catalyst, respectively. Sample 7 was obtained from the fluorination conducted at 340°C for 12 h with the $CrF_3 \cdot 4H_2O$.

Infrared Spectroscopy

The infrared spectra of the catalyst were recorded on a Mattson Infinity FT-IR spectrometer equipped with MCT detector in the range of 1100–4000 cm^{-1} by using vacuum cell (6b–6d) eqipped with CaF_2 windows. The self-supporting disks were prepared by grinding catalyst samples and pressing at 15,000 psi. The catalyst samples in the vacuum cell were outgassed at 10^{-5} Torr for 2 h at 300°C and cooled to room temperature before recording the IR spectrum. Pyridine adsorption experiments were performed by admitting pyridine vapor to the vacuum cell at 50°C and the cell was evacuated at 150°C for 2 h. Adsorption experiments were carried out by flowing CF_3CH_2Cl, $CF_2{=}CHCl$, or other related fluorine-containing compounds into the IR vacuum cell for 0.5 h at a controlled temperature and degassed with N_2 for 0.5 h at 50 and 200°C, respectively.

X-Ray Diffraction (XRD)

A Rigaku (D/Max-III) diffractometer with a nikel-filtered Cu$K\alpha$ excitation source was employed to obtain XRD patterns for all the catalyst samples. The X-ray source was operated at 30 KV and 40 mA with scanning rate 4 deg/min. Compound identification was accomplished by the comparison of measured spectra of the samples with those of reference samples or JCPDS powder diffraction file data.

X-Ray Photoelectron Spectroscopy (XPS)

The XPS measurements were conducted with a VG Scientific ESCALAB 220 spectrometer. The X-ray source with a non-monochromatized Al$K\alpha$ radiation ($h\nu = 1486.6$ eV) was operated at 12.5 KV and 16 mA. The XPS spectra were obtained by a hemispherical energy analyzer with the pass energy of 40 eV and the step of 0.1 eV. Samples 1–4 used in the XPS study were prepared *ex situ* in pellets. The samples were allowed to be outgassed for several hours in the XPS chamber to minimize air contamination to sample surface. No other treatment such as Ar ion sputtering was attempted since it might cause the modification of the composition on the catalysts surfaces. In order to overcome the sample charging problem, the binding energies (B.E.) of core levels in the observed XPS spectra were referenced to the F1*s* core level (B.E. = 685.6 eV) of MgF_2 or C1*s* core level (B.E. = 284.6 eV) of adventitious hydrocarbon (9, 10). The obtained XPS spectra were fitted using a nonlinear square method with the convolution of Lorentzian and Gaussian functions after the polynominal background substraction from the raw spectra (11).

Surface Area

The surface areas were determined by the modified BET method from the adsorption isotherms of nitrogen at liquid nitrogen temperature with the help of the AREA-Meter II.

RESULTS AND DISCUSSION

Activity Study

The fluorination reaction of CF_3CH_2Cl to CF_3CH_2F was studied in a fixed-bed flow reactor.

$$CF_3CH_2Cl + HF \rightarrow CF_3CH_2F + HCl \qquad [1]$$

Table 1 shows that MgF_2-doped chromium fluoride catalyst, sample 1, exhibits much higher catalytic activity in

TABLE 1

Catalytic Activity (mmol h^{-1} g^{-1} cat) of Chromium–Magnesium Fluoride Catalyst Samples 1 to 7 Measured at 340°C (HF/CF_3CH_2Cl = 8/1)

Sample	1	2	3	4	5	6	7
Activity (mmol/h · g-cat)	0.63	0.24	0.03	0.68	0.02	0.01	0.02
Surface area (m^2/g)	69	64	55	73	73	71	8
Carbon content (%)	0.32	1.01	2.98	0.3	0.29	—	—

comparison with undoped chromium fluoride catalyst, sample 7, indicating the important role of MgF_2 in the fluorination of CF_3CH_2Cl. Wojciechowska *et al.* have published numerous reports on the role of MgF_2 in the magnesium fluoride doped metal oxide-catalyzed reactions. They found that the interaction of metal oxide such as MoO_3, Cr_2O_3, and V_2O_5 with MgF_2 generates a considerable increase of the surface area and Lewis acidity (6b–6d). In our previous paper, the use of MgF_2 support is found to be effective in the CrF_3-catalyzed fluorination reaction of CF_3CH_2Cl by enhancing the catalytic activity, suppressing the formation of unwanted side products and lengthening the lifetime of the catalyst (6a). Such an activity enhancement by MgF_2 support can be attributed mostly to the increase in the surface area and acidity (see Fig. 5). However, the electronic interaction of MgF_2 with CrF_3 or the formation of a highly active metal compound such as $MgCrO_xF_y$ cannot be excluded.

The effects of temperature on the catalytic activity are also shown in Table 1 and Fig. 1. Figure 1 shows that the initial catalytic activity increases with the increasing reaction temperature. However, for the reactions carried out at 400 and 450°C, deactivation proceeds very rapidly possibly due to the coke formation. Carbon content was analyzed to correlate the catalytic activity with the extent of coke formation (Table 1). As expected, the more deactivated sample exhibits the higher degree of coke formation, that is, as going from sample 1 to sample 3. Measurements of surface areas also revealed that the higher carbon content, less active catalyst sample shows the smaller surface area. This is obviously due to the fact that cokes formed on the catalyst surfaces block the active sites and catalyst pores resulting in lower activity and smaller surface area. It is noticeable that the catalytic activity is completely recovered after air regeneration of highly deactivated sample 3. These results strongly suggest that carbon deposition on the catalyst surface may be a major factor for the deactivation. The detailed discussion will be given later.

The effect of alkali metal on the catalytic activity was also examined in helping to understand the nature of the active sites for the fluorination reaction. In a brief study, it was observed that addition of 0.5 wt% Li or K to the fluoride catalyst completely quenched the reaction (see Table 1, catalysts 5 and 6) strongly indicating that the active centers are Lewis acid sites. As shown in Fig. 2, the fluorination reaction of CF_3CH_2Cl with HF yielded various side products depending on the reaction temperature. The selectivity to CF_3CH_2F (HFC-134a) decreases with the increasing temperature, whereas the formations of CF_3CHF_2 (HFC-125), CF_2=CHCl (HCFC-1122), and CF_3CH_3 (HFC-143a) increase significantly. The plausible pathways to the side products formation are presented as follows:

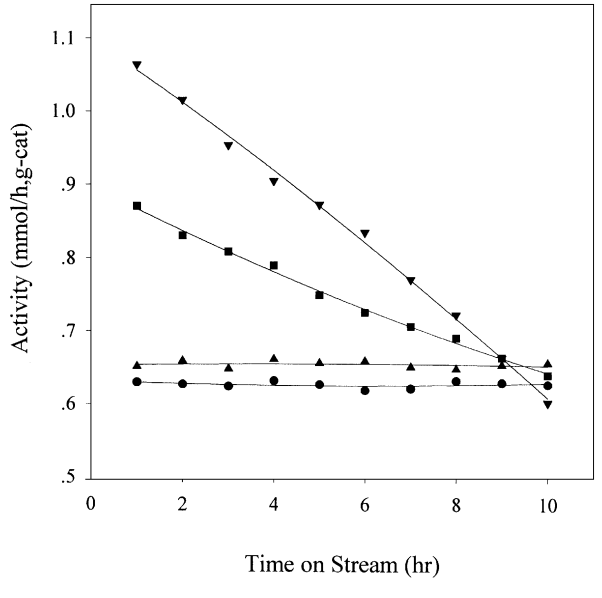

FIG. 1. Performance of catalyst as a function of time on stream (HF : CF_3CH_2Cl = 8 : 1). ●, 340°C; ■, 400°C; ▼, 450°C; ▲, 340°C, after activation.

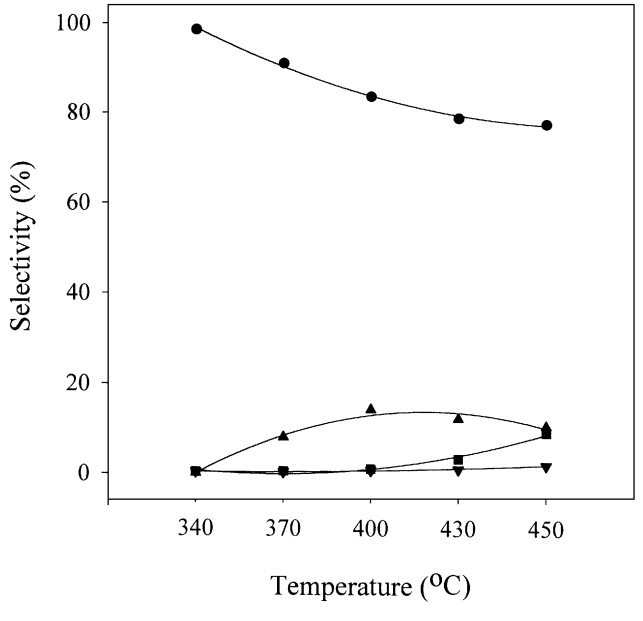

FIG. 2. Variation of selectivity with the reaction temperature (HF : CF_3CH_2Cl = 8 : 1). ●, CF_3CH_2F (HFC-134a); ▲, CF_2=CHCl (HCFC-1122); ■, CF_3CHF_2 (HFC-125); ▼, CF_3CH_3 (HFC-143a).

Cl ↔ F exchange (fluorination)

$$CF_3CH_2Cl + HF \rightarrow CF_3CH_2F + HCl \quad [1]$$

Disproportionation

$$2CF_3CH_2Cl \rightarrow CF_3CHCl_2 + CF_3CH_3 \quad [2]$$

Cl ↔ F exchange (fluorination)

$$CF_3CHCl_2 + 2HF \rightarrow CF_3CHF_2 + 2HCl \quad [3]$$

Dehydrofluorination

$$CF_3CH_2Cl \rightarrow CF_2{=}CHCl + HF \quad [4]$$

For the higher temperature reactions, dehydrofluorination and disproportionation seem to be facilitated. It is interesting to note that the selectivity to $CF_2{=}CHCl$ (HCFC-1122) at 450°C is lower than the selectivity at 400°C. This is probably due to the decomposition of $CF_2{=}CHCl$ (HCFC-1122) into a high molecular weight carbonaceous compound, which is believed to be the precursor of the coke:

$$CF_2{=}CHCl \rightarrow CF{\equiv}CCl \xrightarrow{\text{oligomerize}} \text{Carbonaceous material} \quad [5]$$

The effect of molar ratio of HF/CF_3CH_2Cl on the formation of side products was studied at 340°C in a separate experiment. The amount of side products, CF_3CHF_2, CF_3CH_3, and $CF_2{=}CHCl$ decreases with increasing molar ratio of HF/CF_3CH_2Cl up to 8 suggesting that excess HF are functioning to suppress the formation of side products possibly by tying up the disproportionation and dehydrofluorination sites. Beyond $HF/CF_3CH_2Cl = 8$, however, the amount of side products was nearly independent of the molar ratio of HF/CF_3CH_2Cl indicating the presence of equilibrium.

X-Ray Diffraction

Figure 3 shows XRD patterns of the catalyst samples having different catalytic activities. The XRD results reveal that polycrystalline MgF_2 phase appears in all of the samples while chromium fluoride phase exists in amorphous state. Interestingly, we observed that additional XRD measurements of samples 1–4 after exposing to air for about 2 weeks show the significant appearance of $CrF_3 \cdot 3H_2O$ only in highly active samples 1 and 4. From these results, it is suggested that the catalyst samples contain anhydrous or less hydrated amorphous CrF_3 or CrO_xF_y species which might undergo slow hydration reaction to give crystalline $CrF_3 \cdot 3H_2O$ when contacted with atmospheric H_2O. In the case of deactivated samples 2 and 3, the cokes formed are believed to occupy the active sites at which water molecule can be adsorbed and therefore the formation of $CrF_3 \cdot 3H_2O$ is prohibited. In order to identify the active species, we have performed the fluorination reaction with CrF_3, $CrF_3 \cdot 4H_2O$, $CrF_3 \cdot 3H_2O$, and CrO_xF_y in separate

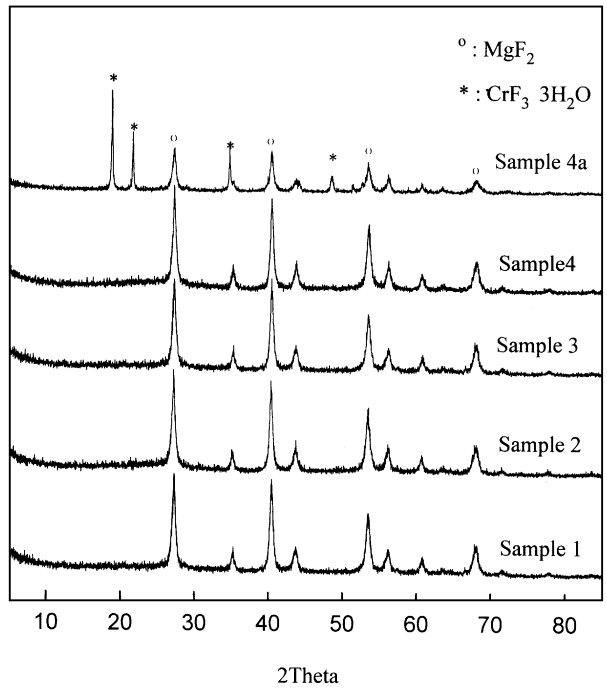

FIG. 3. XRD patterns of samples 1–4 and 4a. 4a, after exposing sample 4 to air for 2 weeks.

experiments. Amorphous CrO_xF_y was obtained from the air calcination of $CrF_3 \cdot 4H_2O$ or $CrF_3 \cdot 3H_2O$ at 400°C for 4 h and is known to have the formula as $CrF_2O_{1/2} \cdot 1/2H_2O$ (4b, 4c). Experimental results that the activity of CrO_xF_y is almost 30 times higher than those of CrF_3, $CrF_3 \cdot 4H_2O$, and $CrF_3 \cdot 3H_2O$ strongly imply that $Cr^{III}F_3$ is not an active species. The effect of water on the catalytic activity was also examined. The presence of H_2O in the feed was found to drastically reduce the catalytic activity. When fluorination reaction was performed at 340°C with CF_3CH_2Cl containing about 2000 ppm H_2O, 70% reduction in activity was observed in 10 h. The original catalyst activity was restored in 2 h on replacing H_2O-containing CF_3CH_2Cl feed by anhydrous CF_3CH_2Cl indicating that H_2O competes with CF_3CH_2Cl for the same active sites. Such a phenomenon is also observed in many other fluorination reactions performed in our laboratory. This might indicate that active sites are located on the surface of chromium fluoride species where H_2O molecules can be adsorbed. However, it is also conceivable that the presence of water in the reactant could reduce the surface fluoride level resulting in lower activity, and higher surface fluoride level may return to their equilibrium values when water feeding is stopped.

IR Study

The IR experiments have been conducted to describe qualitatively the chemical change of chromium compounds on the catalysts in terms of coordinated hydroxyl group. Kijowski *et al.* have reported that the gradual loss of catalyst

activity is associated with a slow and progressive replacement of Cr(III)–O by Cr(III)–F bond (12). In our experiments, the IR spectrum of the catalyst samples 1 to 4 show the broad peak centered at ~3400 cm^{-1} which can be assigned to hydroxyl group in $CrF_x(OH)_{3-x}$ ($x = 1$–2) decreases along the progress of deactivation (spectra are not shown here). From this result we might consider the additional deactivation pathway, beside carbon deposition, due to the decrease in the hydroxyl group in $CrF_x(OH)_{3-x}$ phase which is suspected as another catalytic center.

The hydroxyl group of Brønsted acid site would generate the acid-catalyzed fluorination reaction, depicted as follows, where the interaction of the hydroxyl group with the chlorine of CF_3CH_2Cl causes to weaken the C–Cl bond in CF_3CH_2Cl.

$$-Cr-OH + CF_3CH_2Cl \rightarrow$$
$$Cr-O^{\delta-} \cdots H^{\delta+} \cdots Cl \cdots CH_2CF_3$$

The initial fluorination of chromium hydroxide is intended to increase the Brønsted acidity of remaining OH group, that is, the replacement of the hydroxyl group linked to chromium with fluorine anion weakens the remaining O–H bond due to its strong electronegativity, causing a higher proton mobility. *In situ* IR experiments with CF_3CH_2Cl (HCFC-133a) over sample 4 show that the intensity of the peak corresponding to hydroxyl group of the catalyst decreases as the reaction proceeds, possibly due to the interaction of hydroxyl group with CF_3CH_2Cl (Fig. 4). However,

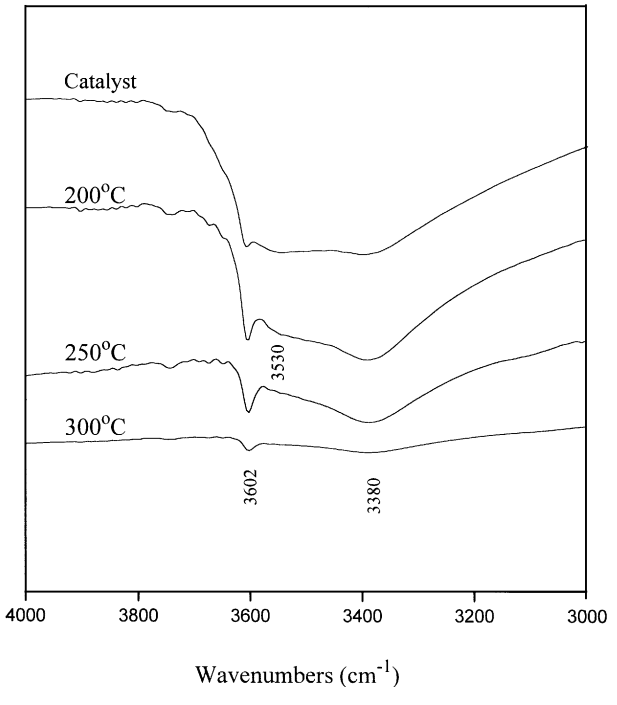

FIG. 4. IR spectra of sample 4 after adsorption of CF_3CH_2Cl at various temperatures.

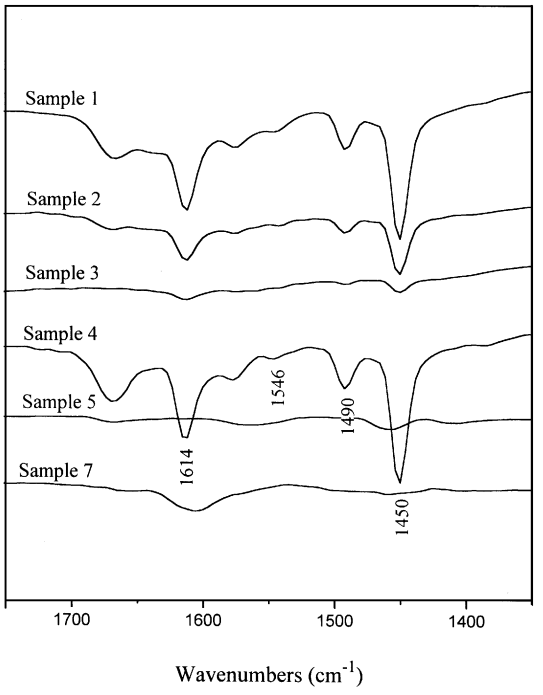

FIG. 5. IR spectra of samples 1–5 and 7 after pyridine adsorption.

at the moment, it is difficult to conclude that such an interaction is related to the catalysis.

It has been proposed that fluorination and disproportionation catalysts must possess Lewis acidity to account for their activities (8). In order to identify Lewis and Brønsted acidity in the catalysts we have performed pyridine adsorption experiments. Figure 5 shows the IR spectra of adsorbed pyridine on the catalyst samples outgassed at 200°C after pyridine adsorption at 50°C. Adsorption bands were observed at 1451, 1540, and 1612 cm^{-1} on all of the samples. The band at 1451 and 1612 cm^{-1} is commonly referred to pyridine coordinatively bound to Lewis acid centers. The band at 1540 cm^{-1} is associated with the pyridinium ion resulting from the interaction of Brønsted acid sites with pyridine molecules (6b–6d). As expected, the intensities of the bands associated with Lewis and Brønsted acidity are extremely weaker for inactive CrF_3 catalyst, sample 7, compared with those for MgF_2-doped catalyst, sample 1, indicating that MgF_2 play an important role in enhancing the catalytic activity by giving Lewis acidity to the CrF_3 catalyst. For the catalyst samples 1–3, the intensities of these bands decrease with increasing reaction temperature, that is, with decreasing activity. The Lewis and the Brønsted acid strength of regenerated sample 4 are almost identical to those of sample 1. The vacant sites of CrF_3 or $CrF_x(OH)_{3-x}$ are believed to be responsible for the Lewis acidity, whereas Brønsted acidity can be attributed to the presence of hydroxyl group. Kijowski *et al.* have also reported a description of fluorination mechanism at a fluorinated chromia surface (12). According to their mechanism, a key of the

catalytic reactions is the existence of labile fluorine produced by the following scheme, which is weakly coordinated to Lewis acidic chromium of CrF_3.

$$\text{HF (weakly adsorbed)} \leftrightarrow \text{catalytically active F} \rightarrow Cr^{III}\text{–F}$$

The vacant sites for the coordination of labile fluorine exist in the coordinatively unsaturated chromium species. In our experiments, the coordinatively unsaturated chromium species are not directly observed. However, as discussed in XRD results, the hydrated chromium phase is thought to represent the coordinatively unsaturated chromium species since the reaction temperature ($\geq$340°C) is high enough for the water molecule to be dissociated from chromium species. In other words, the decrease of hydrated chromium species means the decrease in the coordinatively unsaturated chromium species, prohibiting the coordination of labile fluorine. Therefore, this argument is well consistent with the experimental result that the samples with more hydrated chromium fluoride phase in the spectroscopic analysis demonstrate the greater catalytic activity. On the other hand, the disappearance of coordinatively unsaturated chromium fluoride phases in deactivated samples is likely to be explained by the XPS result that the part of active chromium phase undergo the structural or chemical changes into metal carbides by the interaction with carbon layers during the deactivation process. The correlation between acidity of catalyst and catalytic activity might suggest that both Lewis and Brønsted acid sites are active centers for the Cl–F exchange reaction. As already mentioned, the addition of small amount of alkali metal (0.5%) such as K and Li was found to greatly depress the catalytic activity and also to diminish the intensity of the band at 1451 cm^{-1} corresponding to Lewis acid site indicating that Lewis acidity is a key factor in the fluorination of CF_3CH_2Cl (8). It is reported that catalyst deactivation proceeds via the transformation of Cr–OH to Cr–F after a long period time of reaction in the Cr_2O_3-catalyzed fluorination reaction (12). The importance of the presence of hydroxyl group can be related to Brønsted acidity. However, further studies seem to be needed to determine whether Brønsted acid sites are functioning as the catalytic active centers even though the more active catalyst results in the higher intensity of band at 1540 cm^{-1} indicative of Brønsted acid site.

It is known that the chlorine in the CF_3CH_2Cl is very difficult to replace and thus requires a very high reaction temperature. It is an unfavorable equilibrium reaction. Only about 3% conversion of CF_3CH_2Cl is obtained with stoichiometric amount of HF and CF_3CH_2Cl (13).

$$CF_3CH_2Cl + HF \rightarrow CF_3CH_2F + HCl \quad \Delta H = 18\ \text{kJ/mol}$$

Therefore, a higher molar ratio of HF/CF_3CH_2Cl and reaction temperature are required to increase the conversion. A major problem for this catalysis reaction is the catalyst life. It has been reported that the presence of small amount of oxygen helps to lengthen the catalyst lifetime up to 6 months without any decline in catalyst activity (14). Another major problem is the elimination of HF from CF_3CH_2Cl to give toxic $CF_2{=}CHCl$ (HCFC-1122) which is difficult to remove from the product, CF_3CH_2F (HFC-134a), due to the formation of azeotrope. Formation of $CF_2{=}CHCl$ is considered as a major source of the deactivation since further elimination of HF would lead to coke precursors such as halogenated acetylenes (13). The formation of $CF_2{=}CHCl$ strongly depends on the reaction condition such as molar ratio of HF/CF_3CH_2Cl and reaction temperature.

With the hope of identifying the coke precursor, we have conducted *in situ* FT-IR adsorption experiments with various types of CFCs, HCFCs, and HFCs compound such as CF_3Cl, CF_2Cl_2, $CF_2{=}CH_2$, CF_2HCl, CF_2ClCH_3, and CF_3CH_3 in addition to CF_3CH_2Cl and $CF_2{=}CHCl$ without the presence of HF. Adsorption temperature were varied from 50 to 300°C. After adsorption, the vacuum cell was flushed with N_2 at 50, 200, and 300°C, respectively, and IR spectra were recorded after each desorption at the specified temperature. Unfortunately, we could not able to observe any adsorption of CF_3CH_2Cl below 200°C. However, above 200°C a newly adsorbed species came to emerge whose IR absorption bands are 1592, 1436, and 1259 cm^{-1} (Fig. 6). The newly formed species was difficult to remove from the catalyst surface until air regeneration was performed at 400°C. Interestingly, experiments performed with

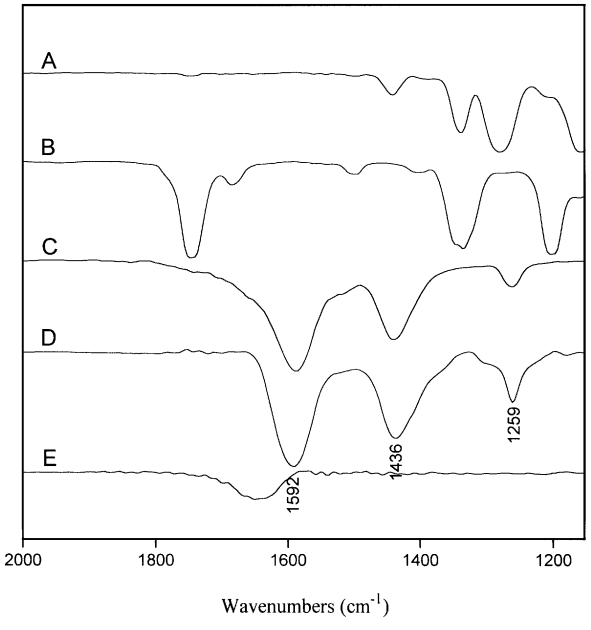

FIG. 6. IR spectra of (A) CF_3CH_2Cl (HCFC-133a); (B) $CF_2{=}CHCl$ (HCFC-1122); (C) catalyst sample 4, after HCFC-133a adsorption at 200°C; (D) catalyst sample 4, after HCFC-1122 adsorption at 150°C; and (E) after air calcination of D at 400°C for 4 h.

CF_2=CHCl yielded the same species, but at lower temperature (150°C). Even though we failed to identify the species, it is believed that the irreversibly adsorbed haloalkane species, coke precursors are formed from the interaction of CF_2=CHCl with strong acid sites. Kemnitz *et al*. reported that CFCs are only weakly adsorbed on the surfaces of certain metal halides and oxides (5c). Therefore, the possible explanation for the failure to detect adsorbed species at lower temperature is likely that weakly adsorbed CF_3CH_2Cl is flushed away by N_2 flow during the process of removing gaseous free CF_3CH_2Cl. Or, the surface coverage of CF_3CH_2Cl is too low to be detected by IR spectroscopy. On the other hand, at a higher temperature, the adsorbed CF_3CH_2Cl species immediately transform into the same species as obtained with CF_2=CHCl, suggesting that CF_2=CHCl could be an intermediate to the coke precursor. The possibility of the formation of one-carbon adsorbed species by the C–C bond cleavage could be ruled out because adsorption IR spectra of CF_3Cl, CF_2Cl_2 and CF_2HCl are completely different from those of CF_3CH_2Cl, CF_3CH_2F, and CF_2=CHCl. At the moment, it seems difficult to conclude whether the adsorption of CF_3CH_2Cl takes place covalently or ionically. However, we may speculate that CF_3CH_2Cl adsorb on the Lewis or Brønsted acid sites covalently or ionically and then lose HF via 1,2-elimination process to give adsorbed CF_2=CHCl species at higher temperature. The adsorbed CF_2=CHCl species again lose HF to give adsorbed acetylenic CF≡CCl species which is easily polymerized to a carbonaceous material, or the adsorbed CF_2=CHCl species may react with neighboring adsorbed CF_2=CHCl species to give unidentified oligomeric species. An effort to characterize the coke precursor is still in progress.

XPS Study

Figure 7 shows the relative concentrations of carbon, chromium and oxygen in the catalyst samples 1–4, which are estimated from the quantification of high resolution XPS spectra. To evaluate the relative concentration, we used the equation

$$\text{Relative concentration for element } i\ (\%) = \frac{a_i/s_i}{\sum_i a_i/s_i} \times 100,$$

where a_i is the area of the peak of chosen core level or element i, and s_i is atomic sensitivity factor for XPS as derived by Wagner (15). It is known that the XPS probes the compositions near the surface region due to the short attenuation length of electrons. The highly deactivated sample 3 shows the decrease of chromium and oxygen concentration in the surface region. On the other hand, the relative concentration of carbon in that sample increases rapidly. This result is consistent with that of elemental analysis which measures

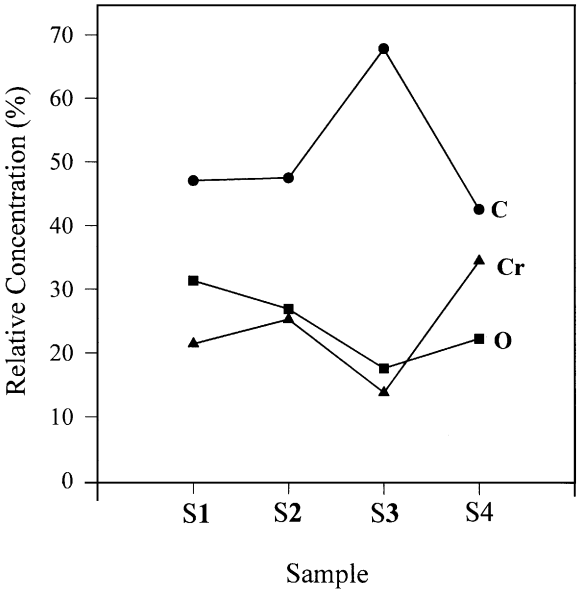

FIG. 7. Relative surface concentration of carbon, chromium, and oxygen for samples 1–4.

total carbon concentration in bulk. The increase in carbon concentration is likely due to the deposition of carbonaceous layer produced by the decomposition of reactants during the fluorination reaction on the catalyst surface. The decrease of the chromium concentration of the deactivated sample 3 in the surface region can be explained by the fact that the chromium surface is covered with carbon layers during deactivation. Also, the decrease of concentration of oxygen can be explained in terms of carbon deposition on the chromium oxide surface and/or substitution of OH with F in chromium species. Figure 7 also shows that, in the reactivated sample 4, the carbon concentration is quite reduced compared to that of the deactivated sample 3 and the relative Cr and O concentrations are recovered, however, somewhat different from those of the fresh catalyst (sample 1), which might be due to compositional change according to the high temperature air calcination for the sample 4.

Cr2*p* core level spectra for samples 1–4 are shown in Fig. 8. The Cr2*p* peak can be deconvoluted with three components for all the samples by a curve fitting procedure. The deconvoluted components are assigned as follows. The high binding energy component at ~580 eV is attributed to CrF_3 (16). The intensity of CrF_3 phase increases slightly as going from sample 1 to sample 3. These species are produced by substituting the hydroxyl group of $Cr(OH)_3 \cdot x(H_2O)$ with fluoride during the activation process and/or fluorination reactions. In addition, the component at ~578 eV is ascribed to $Cr(OH)_3 \cdot x(H_2O)$, and/or $Cr(OH)_xF_y$, where the extent of hydration is not known. The lowest binding energy component at ~576.6 eV is attributed to chromium oxide phase like Cr_2O_3 phase (17). One can notice that the intensity of this chromium oxide component decreases as

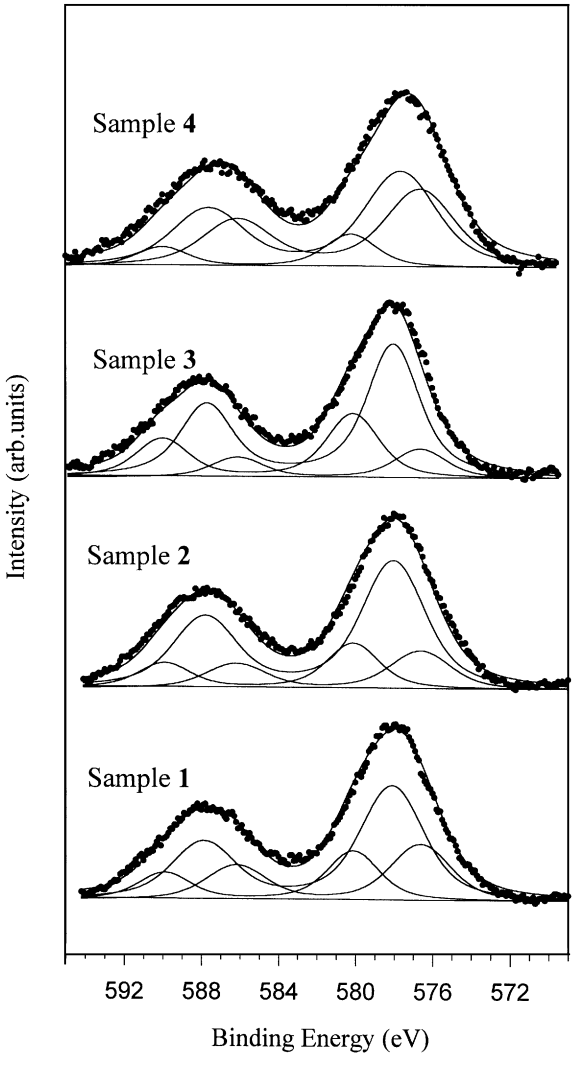

FIG. 8. XPS spectra of Cr2*p* for samples 1–4.

going from sample 1 to sample 3; that is, along with the progress of deactivation while the recovered chromium oxide intensity of the regenerated sample 4 is larger than that of the fresh sample 1 due to the air calcination at high temperature (420°C) as mentioned earlier. This trend of the decrease in chromium oxide phases upon deactivation of the catalysts is also confirmed in the O1*s* core-level spectra of these samples (not shown here), in which the intensity of O1*s* component attributed to chromium oxides also decreases from sample 1 to sample 3. This result indicates that the chromium oxide phases also play a role as an active center as well as the coordinatively unsaturated CrF_3 phases as mentioned earlier.

Figure 9 shows the C1*s* core level spectra of samples 1–4 which show the various peaks at B.E. = 283–288 eV, indicating the existence of various carbon species on the catalyst surface. The curve fitted spectra give rise to four overlapping components for these samples. The deconvoluted components are assigned as follows. The highest binding energy component (B.E. ~289 eV) is ascribed to CHF_x species on the surface (18). The peaks at B.E. ~286.6 eV are also attributed to C–OH species on the surface. In addition, the component at B.E. ~284.6 eV is ascribed to the adventitious hydrocarbon (19). The carbon species of B.E. <284 eV have previously been known as a carbidic carbon associated with a form of atomic carbon such as ≡CH or C_{ads} on various surfaces (283.7 eV on Rh(111) (20), 283.9 eV on Fe(110) (21), 283.8 eV on Fe(100) (22)). These species on the metal surfaces appear to be formed by a hydrogenation reaction in the temperature range of 100–400°C. Therefore, the peak at B.E. ~283 eV which appears to be distinct particularly in the deactivated sample 3 is attributed to carbidic carbon. This peak intensity increases as the deactivation proceeds as going from sample 1 to sample 3. But this feature disappears in the regenerated sample 4. These results may indicate that the main cause of the deactivation of these

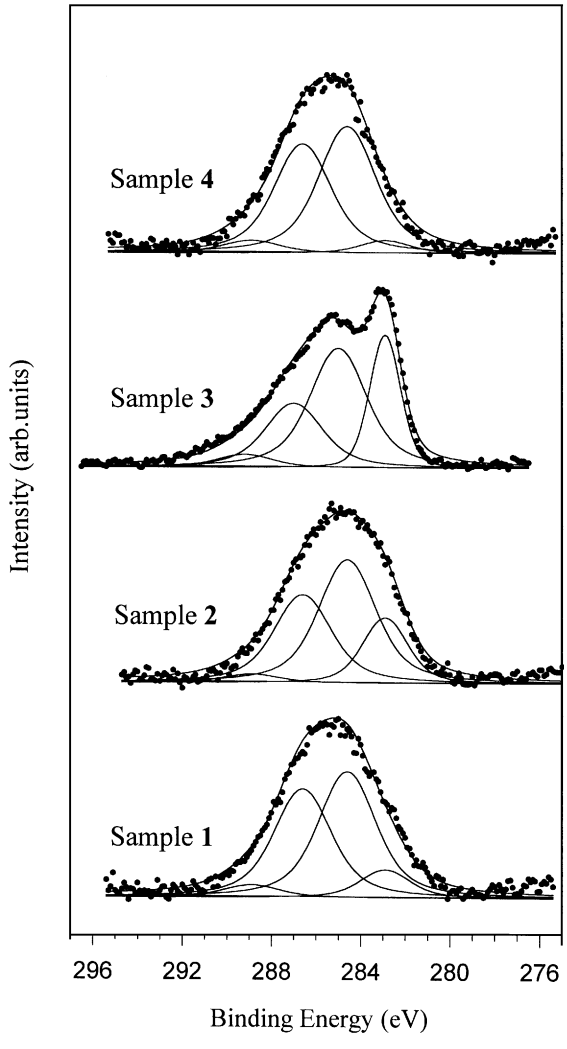

FIG. 9. XPS spectra of C1*s* for samples 1–4.

catalysts is the formation of carbidic carbon on the catalyst surface by decomposition of the reactants during catalysis reaction, that is, carbon coking (23, 24).

The deactivation process has been, in general, divided into four classes which are poisoning carbon coking, sintering, and solid state transformation (25, 26). The deactivation due to poisoning may be negligible in this system, since no impurity occupying the active sites of the catalyst is observed within the detection limit of the Auger electron spectroscopy and XPS. Thermal induced deactivation like sintering or solid state transformations should be considered for the investigation of the deactivation of the catalyst samples, where the catalytically active phases can be converted into the inactive phase. As already mentioned from the experimental results, the chromium species having vacant sites regarded as active centers can be coordinatively saturated as the deactivation proceeds. The interaction between active components and supports are proposed in several other systems (27, 28). Such an interaction also may not be excluded as one of causes of the deactivation of our catalysts. The possibility of sintering of these catalysts accompanying the crystal growth of catalyst phase with the decreasing surface area may not be excluded. Carbon coking might be one of the major causes for the deactivation of the catalyst, where the carbonaceous species encapsulate the catalysts crystallites or the plug pore between support particles. The deactivation of these catalysts will proceed in combination of the processes as mentioned above. However, we can conclude that the main cause of the deactivation for these catalysts is attributed to the carbon coking of the active centers, coordinatively unsaturated chromium species.

CONCLUSION

In summary, the fluorination of CF_3CH_2Cl was performed over chromium–magnesium fluoride catalysts. Initial activity increases with the increasing temperature; however, deactivation was found to proceed fairly rapidly with the reaction time for the higher temperature reactions. The catalyst deactivation was studied by using XRD, IR, and XPS. Pyridine adsorption experiments showed that the catalysts possess both Lewis and Brønsted acid sites of which the strengths diminish with proceeding in deactivation. Addition of alkali metal to the fluoride catalyst was found to quench the reaction showing the important role of Lewis acidity in the catalysis. *In situ* IR studies did not show any appreciable adsorption of CF_3CH_2Cl at the temperature below 200°C, possibly due to the fact that weakly adsorbed CF_3CH_2Cl species is flushed away by He flow during the process of removing gaseous free CF_3CH_2Cl, or the surface coverage of CF_3CH_2Cl is too low to be detected by IR spectroscopy. Instead, irreversible adsorption of newly formed species was observed above 200°C and the same species was also obtained from the $CF_2{=}CHCl$ adsorption experiments conducted at a lower temperature, 150°C. These results suggest that CF_3CH_2Cl loses HF to give $CF_2{=}CHCl$ and the resulting $CF_2{=}CHCl$ immediately transforms into another species which is believed to be a coke precursor.

From the XRD, IR, and XPS results, it is proposed that the active centers are coordinatively unsaturated chromium species which are easily hydrated and the major cause of deactivation is the blocking of the active sites by the coke. Further studies are in progress to elucidate the deactivation phenomena occurring on the catalyst surfaces.

ACKNOWLEDGMENTS

The authors thank Dr. C. Y. Hwang and Y. K. Kim for XPS and XRD measurements.

REFERENCES

1. Webb, G., and Winfield, J., *Chem. Br.* **28**, 996 (1992).
2. (a) Manzer, L. E., *Catal. Today* **13**, 13 (1992); (b) European Patent Application 0446869A1; (c) U.S. Patent 4922037.
3. Coulson, D. R., Wijnen, P. W. J. G., Lerou, J. J., and Manzer, L. E., *J. Catal.* **140**, 103 (1993).
4. (a) Brunet, S., Requieme, B., Matouba, E., Barrault, J., and Blanchard, M., *J. Catal.* **152**, 70 (1995); (b) Japanese Patent Application 52-138084; (c) U.S. Patent 3752850.
5. (a) Hess, A., Kemnitz, E., Lippitz, A., Unger, W. E. S., and Menz, D.-H., *J. Catal.* **148**, 270 (1994); (b) Hess, A., and Kemnitz, E., *J. Catal.* **149**, 449 (1994); (c) Kemnitz, E., Hess, D., and Grimm, B., *Z. Anorg. Chem.* **589**, 228 (1990); (d) Hess, A., and Kemnitz, E., *Appl. Catal. A: Gen.* **82**, 247 (1992).
6. (a) Kim, H., Kim, H. S., Lee, B. G., Lee, H., and Kim, S., *J. Chem. Soc. Chem. Commun.* 2383 (1995); (b) Wojciechowska, M., Gut, W., and Grunwald-Wyspianska, M., *Catal. Lett.* **15**, 237 (1992); (c) Wojciechowska, M., Lomnicki, S., and Goslar, J., *Z. Phys. Chem.* **Bd. 189.S.**, 113 (1995); (d) Haber, J., and Wojciechowska, M., *J. Catal.* **110**, 23 (1988).
7. Ruthruff, R. F., *Inorg. Syntheses* **2**, 190 (1946).
8. Bechadergue, D., Blanchard, M., and Canesson, P., *in* "Heterogeneous Catalysis and Fine Chemicals" (M. Guisnet *et al.*, Eds.), p. 257. Elsevier, Amsterdam, 1988.
9. Murch, G. E., and Thorn, J., *J. Phys. Chem. Solids* **41**, 785 (1980).
10. Wagner, C. D., *J. Electron Spectrosc. Relat. Phenom.* **19**, 1166 (1974).
11. Joyce, J. J., Giudice, M. D., and Weaver, J. H., *J. Electron Spectrosc. Relat. Phenom.* **49**, 31 (1989).
12. Kijowski, J., Webb, G., and Winfield, J. M., *Appl. Catal.* **27**, 181 (1986).
13. Manzer, L. E., *in* "Symposium on the CFC Recycling & Alternatives," p. 159. CMC Co. Ltd., Tokyo, 1988.
14. (a) Japanese Patent Application 2-172933; (b) Japanese Patent Application 1-272535; (c) European Patent Application 0449617A2; (d) U.S. Patent 2030981.
15. Wagner, C. D., *in* "Practical Surface Analysis," Vol. 1, p. 635. Wiley, New York, 1990.
16. Shuttleworth, D., *J. Phys. Chem.* **84**, 1629 (1980).
17. (a) Carver, J. C., Schweitzer, G. K., and Carlson, T. A., *J. Chem. Phys.* **57**, 973 (1972); (b) Battistoni, C., Dormann, J. L., Fiorani, D., Paparazzo, E., and Viticoli, S., *Solid State Commun.* **39**, 581 (1981).

18. Clark, D. T., Feast, W. J., Kilcast, D., and Musgrave, W. K. R., *J. Polym. Sci.* **11**, 389 (1973).
19. Nylund, A., and Olefjord, I., *Surf. Interface Anal.* **21**, 283 (1994).
20. Levis, R. J., DeLouise, L. A., White, E. J., and Winograd, N., *Surf. Sci.* **230**, 35 (1990).
21. Bonzel, H. P., and Krebs, H. J., *Surf. Sci.* **91**, 499 (1980).
22. Panzner, G., and Diekmann, W., *Surf. Sci.* **160**, 253 (1985).
23. Barr, T. L., *in* "Practical Surface Analysis" (D. Briggs and M. P. Seah, Eds.), Vol. 1, pp. 387–389. Wiley, New York, 1990.
24. Somorjai, G. A., and Zaera, F., *J. Phys. Chem.* **86**, 3070 (1982).
25. Forzatti, P., Buzzi-Ferraris, G., Morbidelli, M., and Carra, S., *Int. Chem. Eng.* **24**, 60 (1984).
26. Bartholomew, C., *Chem. Eng.* **91**, 96 (1984).
27. Ronald, M. H., and Farrauto, R. J., *in* "Catalytic Air Pollution Control," p. 67. Thompson, Washington, DC, 1995.
28. Satterfield, C. N., *in* "Heterogeneous Catalysis in Industrial Practice," p. 102. McGraw–Hill, New York, 1991.